Materials Science Forum
ISSN: 1662-9752, Vol. 1187, pp 113-119
doi:10.4028/p-5Dfi7O

Submitted: 2025-12-18
Revised: 2026-02-10
Accepted: 2026-02-17
Online: 2026-04-17

Development of an Initial FEM Framework to Model Particle-Substrate Contact in Fluidized Bed Finishing of L-PBF Parts

Viscusi Antonio[1,a*], El Hassanin Andrea[2,b] and Squillace Antonino[2,c]

[1]Department of Engineering and Sciences, Faculty of Technology and Innovation Sciences, Universitas Mercatorum, Piazza Mattei 10, 00186 Rome, Italy

[2]Department of Chemical, Materials and Production Engineering, University of Naples Federico II, P.le V. Tecchio 80, 80125 Napoli, Italy

[a*]antonio.viscusi@unimercatorum.it, [b]andrea.elhassanin@unina.it, [c]squillac@unina.it

*corresponding author

Keywords: numerical study, fluidized bed, surface finishing, laser-powder bed fusion.

Abstract. This work introduces an initial finite element (FE) framework for modelling particle-substrate interaction during fluidized bed surface finishing of Laser Powder Bed Fusion (L-PBF) components. Due to the complexity of as-built surface morphology and the difficulty of experimentally observing high-speed particle impacts, the mechanisms governing material removal remain poorly understood. The proposed 3D explicit FE model simulates the impact of stainless-steel particles on representative AlSi10Mg asperities using Johnson-Cook plasticity model and damage formulations. Results show that erosion occurs mainly through localized brittle-like detachment rather than extensive plastic deformation. Sequential impacts and oblique trajectories significantly increase internal energy absorption, enhancing asperity fragmentation and the surface smoothing level. The framework provides a foundation for future optimization of Fluidized Bed Finishing (FBF) parameters for improved finishing of additively manufactured metal parts.

Introduction

Additive Manufacturing (AM), commonly known as 3D printing, has evolved from a rapid-prototyping tool into a viable production technology capable of creating fully functional metal components [1]. Among metal AM processes, Powder-Bed Fusion - particularly L-PBF - has gained significant industrial and research interest due to its ability to produce complex geometries directly from digital models [2]. Despite its advantages in design freedom, time reduction, and cost efficiency, L-PBF still presents challenges such as porosity, cracking, spatter formation, and poor surface quality [3].

Surface roughness in L-PBF parts is typically quite higher than that of machined surfaces due to balling effects, partially fused particles and staircase-effect, making post-processing essential [3]. Conventional finishing techniques often struggle with the intricate shapes enabled by AM, motivating alternative approaches [4]. FBF has emerged as a promising solution, offering uniform abrasive action on complex components. Previous studies indicate that abrasive particle density, shear-flow conditions, and removal of partially sintered surface particles strongly influence finishing performance [5]. However, the physical mechanisms governing particle-surface interaction remain difficult to observe experimentally due to the small spatial and temporal scales involved. Numerical modelling can therefore provide valuable insights.

Several researchers have employed the finite element methods for the simulation of the process of solid particle erosion that occurs in abrasive machining [6-10]; however, to the authors best of knowledge, no finite element studies currently address FBF of L-PBF metal parts.

The aim of this study is to establish the first FE modelling framework dedicated to describing particle-substrate contact during FBF of L-PBF specimens produced. As no previous numerical investigations exist on this topic, this initial FE approach is conceived as a foundational step toward understanding the micromechanical interaction mechanisms that govern abrasive material - substrate interaction. The framework is intended to provide a scientific basis for future model refinement and

to support the optimization of FBF process parameters for complex additively manufactured metal parts.

Numerical Procedure

In this section, a 3D finite element model is introduced to simulate the particle-substrate interaction occurring during fluidized-bed surface finishing of additively manufactured metal components, using the commercial FEA software Abaqus. The following subsections detail the adopted geometry and material modelling assumptions.

Geometrical properties.

The experimental campaign was conducted on 20 × 20 × 2 mm³ square specimens produced vertically on the build plate using an EOS EOSINT M280 L-PBF system and AlSi10Mg feedstock powder supplied by EOS GmbH. The case study related to the FE modeling setup described as follows refers to the best FBF condition observed experimentally elsewhere [5], in which a relative speed between the fluidized particles and the substrate was set at 2 m/s through a rotation-assisted finishing process configuration. The FBF was performed using steel particles with nominal mean diameter $d_p = 500\ \mu$m.

For modelling purposes, the finishing mechanism was idealized as the sliding of a single spherical particle over the substrate, striking an individual surface asperity at a given velocity, which is equal to the experimental one. Still for the sake of simplicity, a spherical shape was assumed instead of the irregular or the cut wire ones selected for the experimental work on which this study is based [5], selecting then the nominal value of the mean diameter reported above. The geometry of asperity was defined based on statistical measurements obtained from SEM (HITACHI TM3000) analyses of the as-built surfaces [5] and represented as a conical feature with height $d_p/20$ and base diameter $d_p/4$. A schematic of the adopted in-plane geometric configuration for the FE model is presented in Fig. 1.

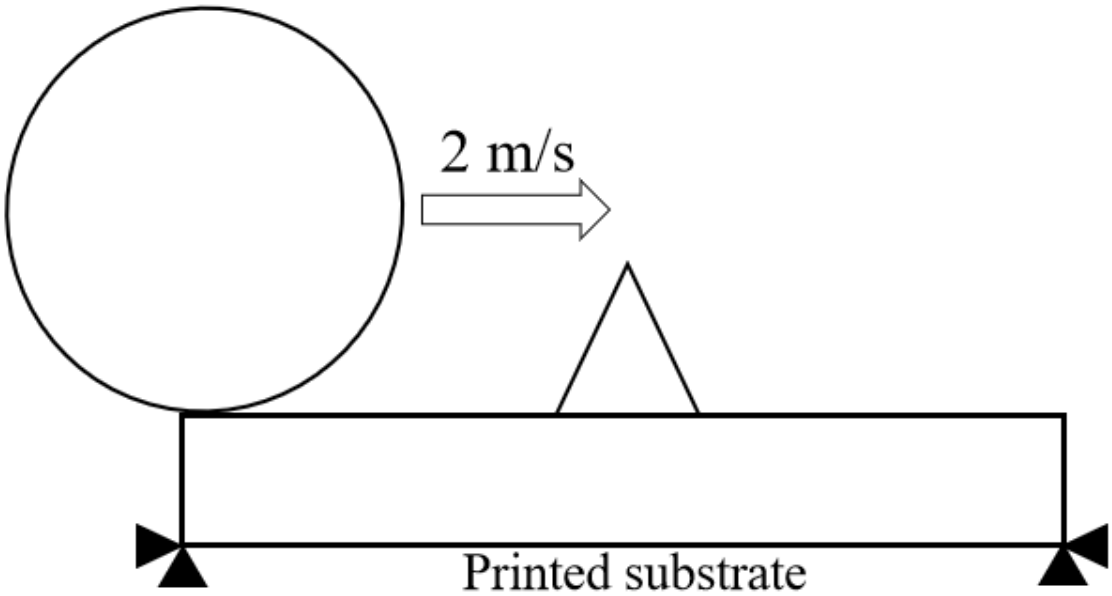

Fig. 1. 2D-Schematization of geometry employed for FE development.

Both the particle and the substrate were represented using a Lagrangian reference frame. The numerical simulations employed an explicit dynamic formulation with geometric nonlinearity enabled.

The particle and substrate domains were discretized using 8-node linear brick elements with reduced integration and hourglass control (C3D8R). A nominal mesh size of *dp*/10 was applied to

both the particle and the substrate. To balance solution accuracy with computational efficiency, the geometries of both bodies were partitioned into multiple regions to allow local mesh refinement in the particle-substrate interaction zone. Within this refined region, the particle was meshed with an element size of *dp*/50 and the substrate with *dp*/200.

The lower surface of the substrate was fully constrained in all degrees of freedom, while symmetry boundary conditions were applied on the x-y plane faces of both the particle and the substrate. Contact interactions were modeled using the *General Contact* algorithm. A friction coefficient of 0.3 [11] was prescribed at all potential contact interfaces.

An initial particle velocity of 2 m/s was assigned. The temperature of both the substrate and the particle (assumed to be at room temperature (298 K)) was assumed as starting conditions. The complete three-dimensional FE model is depicted in Fig. 2.

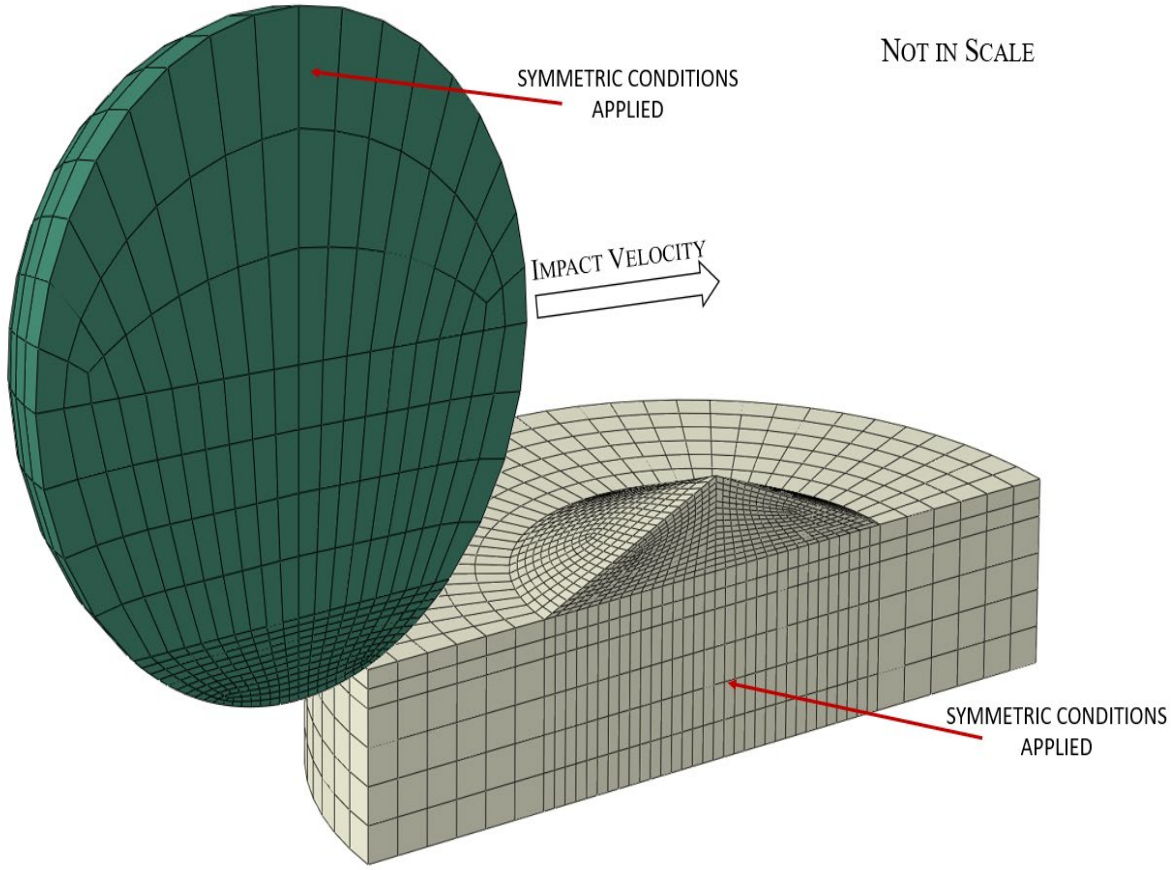

Fig. 2. 3D FE model of an AlSi10Mg substrate with a cone-shaped surface asperity impacted by a spherical steel particle.

Materials modelling.

A bilinear elastoplastic material model with isotropic hardening was assigned to the steel particle. For the AlSi10Mg substrate, the Johnson-Cook (J-C) plasticity model was employed.

The J-C parameters for AlSi10Mg material were determined by combining experimental and literature data. First, specimens of the printed material were characterized by tensile tests applying the load along the building direction, according to ASTM E8 Standard Test Method; then, starting from literature [12], the J-C parameters were properly calibrated on the experimental curve, under low strain rate conditions ($\dot{\varepsilon} \approx 10^{-3} s^{-1}$).

The J-C failure model was employed to predict the onset and the evolution of failure with the material constants taken from literature [13].

In summary, the material properties employed for FE modelling development for both the particle and the substrate are reported in Table 1.

Table 1. Material parameters employed for FE modelling.

Material parameter	AlSi10Mg	416 SS
Density, [kg/m^3]	2700	7600
Young's modulus, [GPa]	70.0	200
Poisson ratio	0.33	0.20
Yielding stress [MPa]		275
Ultimate tensile stress [MPa]		515
Thermal conductivity, [W/m °C]	204	
Heat capacity, [J/kg·°C]	904	
Inelastic heat fraction	0.9	
Melting temperature, [K]	860	
J-C parameter, A, [MPa]	250	
J-C parameter, B, [MPa]	1730	
J-C parameter, n	0.68	
J-C parameter, C	0.0166	
J-C parameter, m	1.571	
J-C damage constant, d_1	0.04704	
J-C damage constant, d_2	1.155	
J-C damage constant, d_3	-0.841	
J-C damage constant, d_4	-0.842	
J-C damage constant, d_5	0	
Reference strain rate, $\dot{\varepsilon}_0$, [s^{-1}]	0.001	
Reference temperature, T_R, [K]	298	

Results and Discussion

Fig. 3 illustrates the erosion pattern generated by the impact of a single particle. The simulation reveals that material removal occurs predominantly through localized element deletion, rather than through significant plastic deformation of the substrate.

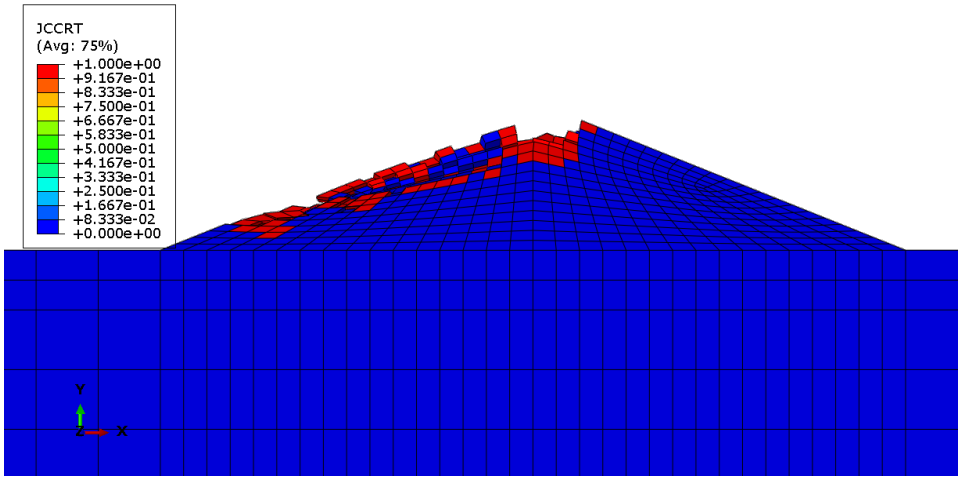

Fig. 3. Material erosion following single-particle impact. JCCRT is Johnson-Cook Cumulative Damage Criterion.

This behavior suggests that the smoothing effect observed is primarily driven by brittle-like detachment of partially sintered asperities characteristic of L-PBF surfaces [3]. The absence of extended plastic zones further confirms that the impact energy is concentrated within a narrow region, promoting surface leveling through micro-fragmentation rather than plastic surface re-modeling.

To investigate the cumulative effect of repeated collisions, the internal energy absorbed by the substrate was evaluated for one and two consecutive particle impacts. As shown in Fig. 4, the second impact contributes substantially to the overall energy input, producing an increase of approximately 60% with respect to the single-impact condition. This enhanced energy absorption correlates with greater material removal, indicating that sequential particle interactions serve to progressively weaken the surface asperities.

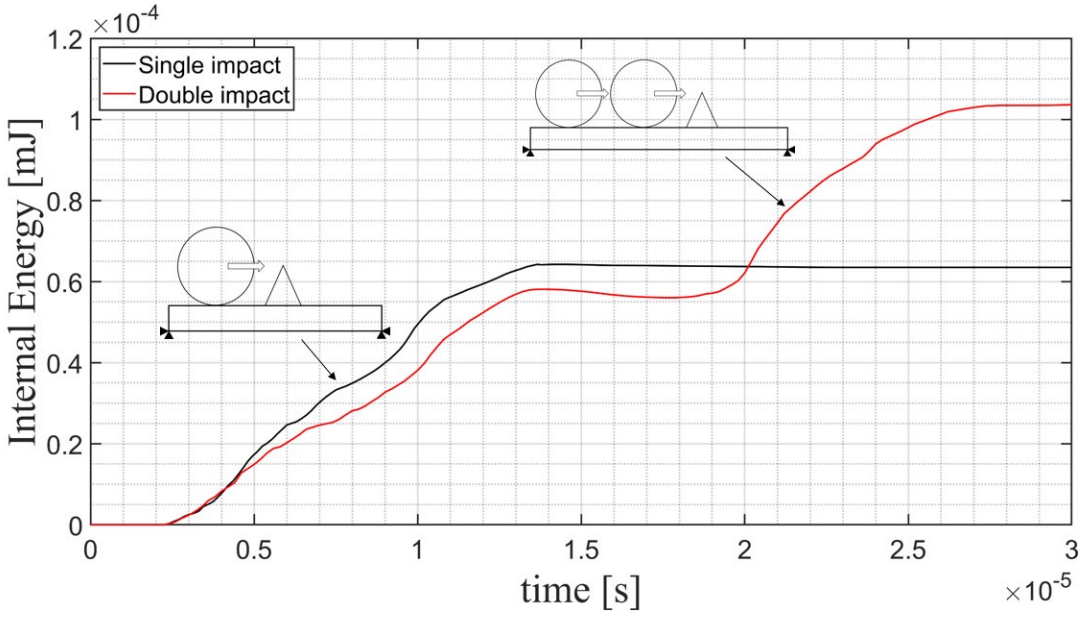

Fig. 4. Internal energy evolution of the substrate under single and double particle impacts.

The influence of particle incidence angle on material erosion was examined through a single-particle impact at 25° relative to the horizontal surface, as reported in Fig. 5.

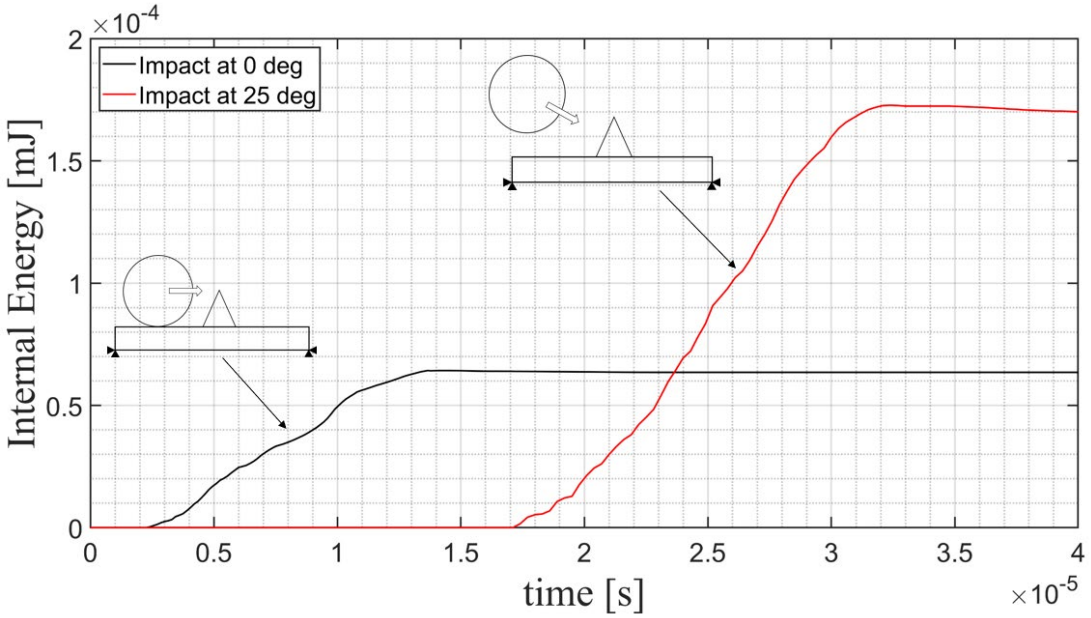

Fig. 5. Internal energy response of the substrate during a single particle impact and at a 25° incident angle.

Introducing an oblique trajectory significantly increases internal energy of substrate, reaching roughly 1.7×10^{-4} mJ, corresponding to an enhancement of about 170% compared with the "normal" impact case. This result indicates that angled impacts are more effective in generating surface erosion due to their ability to combine normal and tangential loading, which improves crack initiation and propagation along surface irregularities.

Finally, the combined effect of multiple impacts and varying impact angles was analyzed, and the results are summarized in Fig. 6. When the substrate is subjected first to a "normal" impact and subsequently to an impact at 25°, the internal energy reaches its maximum value of approximately 2.3×10^{-4} mJ. This configuration produces the most pronounced erosive effect among all tested conditions, demonstrating a synergistic interaction between the initial weakening of the surface by "normal" impact and the intensified removal produced by the angled impact. These findings suggest that, in practical FBF operations, rotating or oscillating the specimen to expose the surface to a range of angles could significantly enhance finishing efficiency.

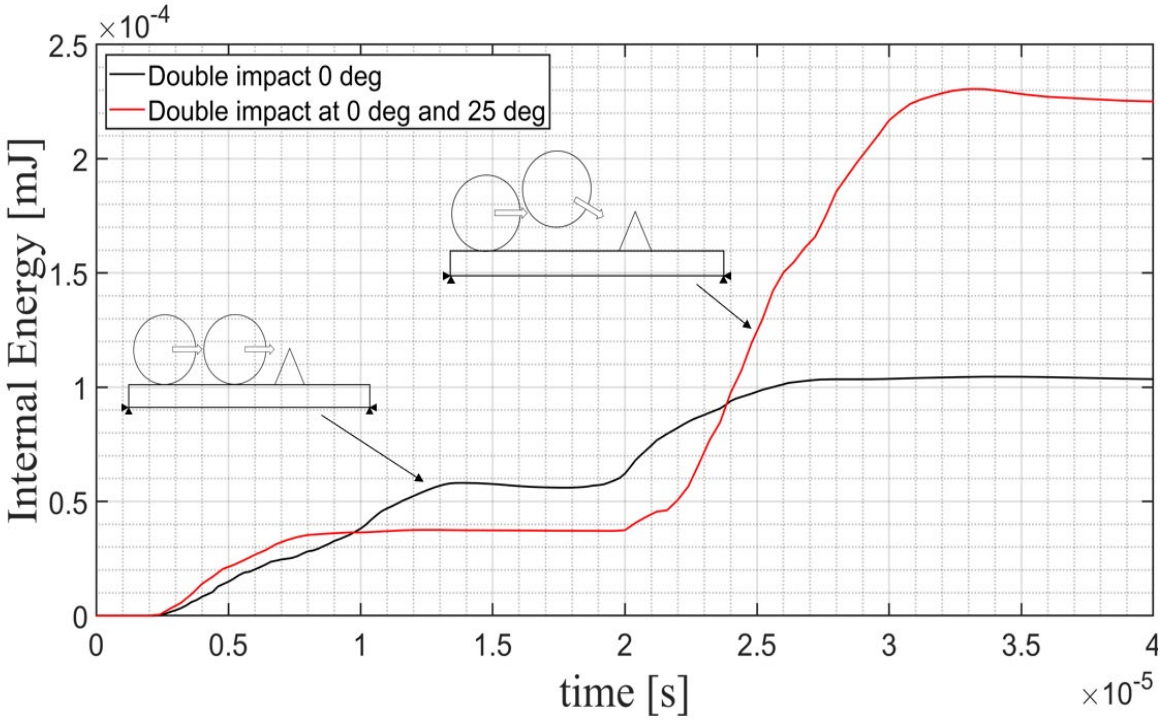

Fig. 6. Internal energy comparison for two sequential impacts: both at 0° and at combined angles (0° followed by 25°).

Conclusion

Based on the results obtained, the following conclusions can be drawn:

- Material removal is dominated by localized brittle-like detachment of surface asperities, not by significative plastic deformation.
- A second particle impact increases internal energy by ~60%, promoting progressive weakening and erosion.
- Oblique impacts (25°) enhance erosion efficiency by raising internal energy by ~170% compared with "normal" impacts.
- Combining "normal" and oblique impacts yields the highest erosion, demonstrating a synergistic removal mechanism.

These findings suggest that varying the incident angle-e.g., through specimen rotation in FBF could significantly improve finishing performance. For subsequent models, the authors intend to develop a more realistic representation of surface morphology, including multiple asperity geometries and non-spherical abrasive particles.

References

[1] Armstrong, M., Mehrabi, H., and Naveed, N., An overview of modern metal additive manufacturing technology, J. Manuf. Process. 84 (2022) 1001–1029.

[2] Chowdhury, S., Yadaiah, N., Prakash, C., Ramakrishna, S., Dixit, S., Gupta, L. R., et al., Laser powder bed fusion: a state-of-the-art review of the technology, materials, properties & defects, and numerical modelling, Journal of Materials Research and Technology 20 (2022) 2109–2172.

[3] DebRoy, T., Wei, H. L., Zuback, J. S., Mukherjee, T., Elmer, J. W., Milewski, J. O., et al., Additive manufacturing of metallic components – Process, structure and properties, Prog. Mater. Sci. 92 (2018) 112–224.

[4] Lee, J. Y., Nagalingam, A. P., and Yeo, S. H., A review on the state-of-the-art of surface finishing processes and related ISO/ASTM standards for metal additive manufactured components, Virtual Phys. Prototyp. 16 (2021) 68–96.

[5] Troiano, M., El Hassanin, A., Solimene, R., Silvestri, A. T., Scala, F., Squillace, A., et al., Fluidized bed finishing of additively manufactured objects: The influence of operating parameters, Powder Technol. 432 (2024).

[6] Pradhan, K.K.; Chakraverty, S., Generalized power law exponent based shear deformation theory for free vibration of functionally graded beams. Applied Mathematics and Computation 268 (2015) 1240–1258.

[7] Feng, Y., Jianming, W. & Feihong, L. Numerical simulation of single particle acceleration process by SPH coupled FEM for abrasive waterjet cutting. Int J Adv Manuf Technol 59 (2012) 193–200.

[8] Jayswal, S., Jain, V. & Dixit, P. Modeling and simulation of magnetic abrasive finishing process. Int J Adv Manuf Technol 26 (2005) 477–490.

[9] Kumar, G.; Yadav, V. Temperature distribution in the workpiece due to plane magnetic abrasive finishing using FEM. Int. J. Adv. Manuf. Technol. 41 (2009) 1051–1058.

[10] Chaieb, I., Ben Moussa, N., Ben Fredj, N. et al. An innovative contactless finite element simulation of the shot peening process. Int J Adv Manuf Technol 113 (2021) 2121–2136.

[11] Yildirim B, Fukanuma H, Ando T, Gouldstone A, Müftü S, A numerical investigation into cold spray bonding processes. J Tribol 137 (2015):011102.

[12] Akturk, M., Boy, M., Gupta, M.K., Waqar, S., Krolczyk, M.G., Korkmaz, M.E., Numerical and experimental investigations of built orientation dependent Johnson-Cook model for selective laser melting manufactured AlSi10Mg, J. Mater. Res. Technol. 15 (2021) 6244–6259.

[13] Cai, X., Pan, C., Wang, J., Zhang, W., Fan, Z., Gao, Y., Xu, P., Sun, H., Li, J., Yang, W., Mechanical behavior, damage mode and mechanism of AlSi10Mg porous structure manufactured by selective laser melting, J. Alloys Compd. 897 (2022) 162933.